http://dx.doi.org/10.5012/bkcs.2012.33.8.2675

Formation of Niobium Oxide Film with Duplex Layers by Galvanostatic Anodization

Hyun-Kee Kim,[a] Jeong Eun Yoo,[†,a] Jiyoung Park,[†] Eul Won Seo,[*] and Jinsub Choi[†,*]

Department of Biological Science, Andong National University, Andong 760-749, Korea. [*]E-mail: ewseo@andong.ac.kr
[†]Department of Chemical Engineering, Inha University, Incheon 402-751, Korea. [*]E-mail: jinsub@inha.ac.kr
Received April 2, 2012, Accepted May 15, 2012

Studies on niobium anodization in the mixture of 1 M H_3PO_4 and 1 wt % HF at galvanostatic anodization are described here in detail. Interestingly, duplex niobium oxide consisting of thick barrier oxide and correspondingly thick porous oxide was prepared at a constant current density of higher than 0.3 $mAcm^{-2}$, whereas simple porous type oxide was formed at a current density of lower than 0.3 $mAcm^{-2}$. In addition, simple barrier or porous type oxide was obtained by galvanostatic anodization at a single electrolyte of either 1 M H_3PO_4 or 1 wt % HF, respectively. The formation mechanism of duplex type structures was ascribed to different forming voltages required for moving anions.

Key Words : Niobium, Porous layer, Barrier layer, Duplex oxide

Introduction

Various cost-effective methods, such as the sol-gel method and gas phase deposition, have been developed to produce niobium oxide with controllable morphologies because of its various applications such as ferroelectric compounds,[1] dye solar cells,[2,3] implants,[4,5] biosensors,[6] capacitors,[7,8] and photocatalysts.[9,10] Among them, the anodization of a niobium foil has been considered a powerful technique for the mass-production of niobium oxide films with various nanostructures on a substrate. For example, the formation of niobium oxide consisting of pores,[11,12] or microcones,[13] and electrochemically-etched niobium structures[8] by anodization (or electrochemical etching) has been reported recently. In addition, we have demonstrated that niobium oxide nanopowders consisting of round and needle shape nanoparticles can be prepared through anodization in ethylene glycol containing NH_4F at a high voltage.[14] The basic idea for the formation of nanopowders was attributed to the mechanism of breakdown and build-up of oxide at a high constant voltage and chemical etching.

Typically, the above-mentioned nanostructures have been prepared by a constant voltage mode (potentiostatic anodization) since the pore diameter, interpore distance, sizes of microcone and etched structures are strongly influenced by the applied voltage.[12-15] Anodization at a current mode (galvanostatic anodization) has been mainly applied to study growth kinetics,[16,17] control of local catastrophic phenomena[18,19] or self-ordered structures in anodization of aluminum[20,21] and to produce TiO_2 nanotubes with periodical morphology.[22] However, there have not been many reports on the anodization of other valve metals by galvanostatic anodization.

In this report, for the first time, we demonstrate that anodization of niobium by galvanostatic anodization can produce duplex oxide layers consisting of a thick porous layer as well as a thick barrier oxide layer. We found that usage of a mixture of electrolytes as well as high current density is required for the production of the duplex oxide layers. The formation mechanism requirements are further described in detail. As known, mechanical and chemical properties such as corrosion resistance, wear resistance, adhesion for paint primers and coloring can be dramatically influenced by the nanostructures of oxide formed on metals. Thus, we expect that the duplex oxide layer can provide a chance to functionalize the metal surface.

Experimental

Nb foils (99.9% purity), with a thickness of 0.25 mm, were purchased from Goodfellow (England). Deionized water (DI water, >18 MΩ) was used to prepare an aqueous mixture solution of 1 wt % HF and 1 M H_3PO_4. The Nb foils were ultrasonicated in acetone for 5 min, washed with ethanol, and dried with a stream of N_2 gas.

The Nb foils were anodized under a constant current density in the range of 0.05 $mAcm^{-2}$ to 1 $mAcm^{-1}$ in the mixture of 1 wt % HF and 1 M H_3PO_4 at room temperature, using a potentiostat/galvanostat (AutoLab PGSTAT12, Eco Chemie) interfaced to a computer.

The cell was a three-electrode system consisting of a Pt mesh acting as the counter electrode, Ag/AgCl/3 M KCl as the reference electrode and a 1 cm^2 Nb foil as the working electrode. During the electrochemical anodization, the stirring rate of the electrolyte remained constant (~180 rpm).

The surface morphologies and thickness of the anodized niobium were characterized by a field emission scanning electron microscope (FE-SEM, 4300S). For the cross sectional view, the backside of the sample was deeply scratched by a diamond cutter (Metsaw^{TM}) and subsequently was mechanically bent.

[a]These authors contributed equally to this work and both should be considered as first authors.

Results and Discussion

Figure 1 shows top view SEM images of porous niobium oxide structures, which were prepared using different constant current densities. At first glance, we can observe three distinct features: nanosized pores, line boundaries, and large holes. In general, nanosized pores were produced using the local dissolution of a formed oxide layer via anodization of niobium at constant voltage in an electrolyte containing F^- ions.[12] Thus, the formation of nanosized pores is attributed to the anodization of niobium in an electrolyte containing F^- ions. Line boundaries probably originated from grain boundaries in the metal surface, where pores are easily nucleated because of high surface energy. We assumed that the large holes were attributed to the collapse of nanosized pores due to massive ionic movement. The following section discusses this in detail.

Figure 2 shows the SEM images of cross-sectional views of the samples shown in Figure 1. A typical porous type oxide consisting of a very thin barrier oxide layer on the bottom of the thick porous layer, which is generally observed in potentiostatically prepared anodic films, is exhibited in Figure 2(a) and (b).[12] In the case of potentiostatic anodization, the barrier oxide layer thickness was determined by the applying voltage, and the porous oxide layer thickness was typically dependent on the anodizing time.[23]

Figure 2 suggests that the higher the current density applied, the thicker the films grow. Interestingly, as the current density increased, both the porous and barrier oxides grew significantly. To the best of our knowledge, a thick duplex film consisting of porous and barrier oxide layers has been not yet reported. Regardless of anodization mode

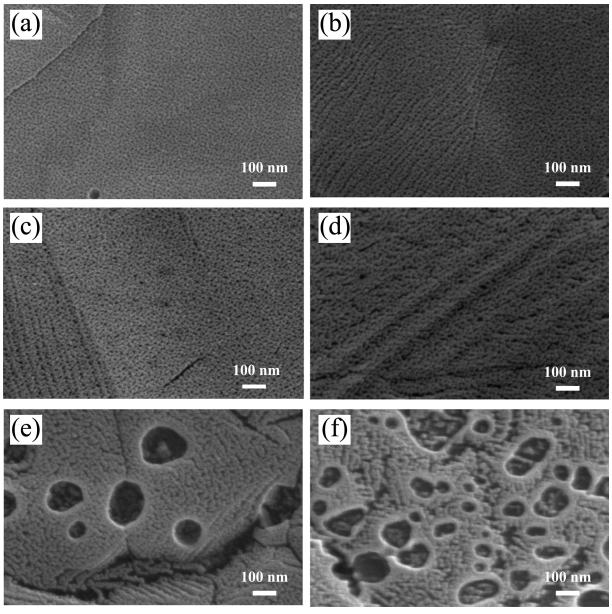

Figure 1. FE-SEM images of the top view of the porous niobium oxide formed by galvanostatic anodization in a mixture of 1 M H_3PO_4 and 1 wt % HF for 1 h at room temperature at current density of (a) 0.1 $mAcm^{-2}$ (b) 0.2 $mAcm^{-2}$ (c) 0.3 $mAcm^{-2}$ (d) 0.4 $mAcm^{-2}$ (e) 0.6 $mAcm^{-2}$ and (f) 0.7 $mAcm^{-2}$.

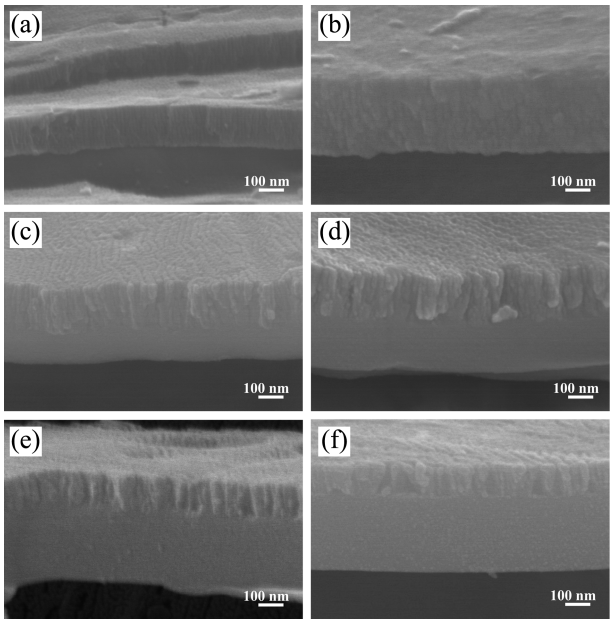

Figure 2. Cross-sectional FE-SEM images of the porous niobium oxide formed by galvanostatic anodization. Figs. 2(a)-(f) corresponds to Figs. 1 (a)-(f).

(either potentiostatic or galvanostatic), we found that only either barrier oxide or porous oxide, with a highly-dissolved surface, was formed in the single H_3PO_4 or in the single HF, respectively.[12] Figure 3 shows the thickness of the porous layer, barrier oxide layer, and total oxide layers, respectively, as a function of applying current density in the mixture of 1 M H_3PO_4 and 1 wt % HF, showing that the thickness of the total and barrier layers increased as current density increased. On the other hand, the thickness of the porous layer decreased. This strongly indicates that an increase in the total thickness is attributed to an increase in thickness of the barrier layer, which is determined by voltage as mentioned above.

Since the duplex structure has not been observed in a

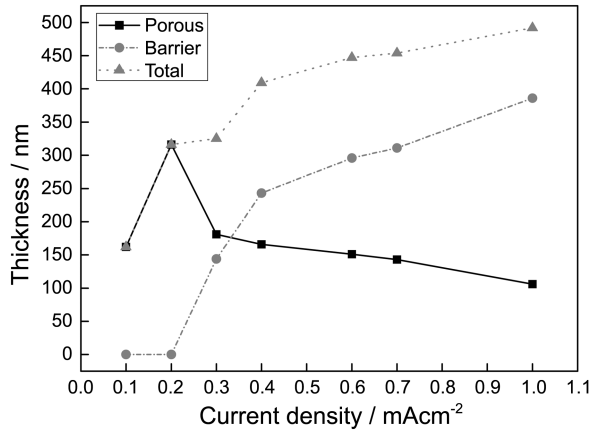

Figure 3. Thickness changes of the porous, barrier and total layers as a function of current density. Note that anodization is carried out in the mixture of 1 M H_3PO_4 and 1 wt % HF for 1 h at room temperature.

single acidic solution or at a low current density, we can conclude that the mixture electrolyte at a high current density plays a primary role in the formation of the duplex structure. As the film thickness increases at a constant current density, the voltage formed between the electrodes (herein, called "forming voltage") increases. Both PO_4^{3-} and F^- anions actively work for the formation of the barrier oxide and porous oxide, respectively, if the forming voltage is higher than a critical value. It is due to the relatively higher forming voltage required to move heavy PO_4^{3-} ions, compared to F^- ions, through the film. On the other hand, if low current density, which does not lead to critical value achievement of the forming voltage, is applied, F^- ions mainly contribute to the formation of the porous oxide and the PO_4^{3-} ions are competitively adsorbed on the surface to protect the oxide film from dissolution by the aggressive F^- ions.[12]

As expected, formation of either typical porous type oxide or duplex oxide exhibits different voltage transients (Fig. 4). For example, the current densities of 0.05 $mAcm^{-2}$, 0.1 $mAcm^{-2}$, and 0.2 $mAcm^{-2}$ show almost constant voltages, being independent of anodizing time, producing the porous-type oxide. However, duplex oxides that are formed at higher than 0.3 $mAcm^{-2}$ exhibit linear slopes of voltages in terms of anodizing time. The slope of voltage *vs.* time increases with increased current density. A higher maximum voltage is observed at a higher current density. Since the thickness of the barrier oxide layer is linearly proportional to the maximum voltage, the greater thickness of films at a higher current density is attributed to higher achievement of maximum voltage (Fig. 4(b)). Subsequently, a sudden drop in voltage is observed, and the time required for the sudden drop in voltage shortens when the current density increases. Since the voltage drop indicates a current leakage, we suppose that the sudden drop in voltage is ascribed to the breakdown of barrier oxide. In addition, since massive ions move through the oxide films, the formed oxide is highly dissolved at higher current density. This results in the formation of large holes by the collapse of nanosized pores. It is easily observed at a current density of higher than 0.3 $mAcm^{-2}$.

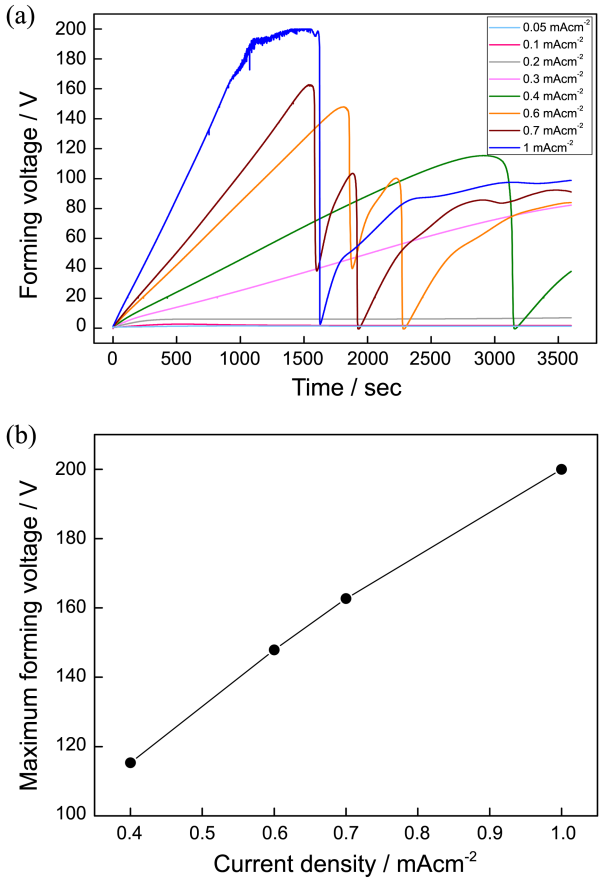

Figure 4. (a) Forming voltage transients as a function of anodization time. Anodization at low current densities (< 0.3 $mAcm^{-2}$) shows relatively constant forming voltage transients, whereas the forming voltage linearly increases as the anodization proceeds at high current densities (> 0.3 $mAcm^{-2}$) (b) the relationship between the maximum forming voltage and applied current density.

Table 1 shows the summary of oxide thickness in terms of current density and anodizing time. As expected, the greater the voltage applied, the greater the total thickness formed in the same anodizing time. For example, thickness of 325, 409, 447, 454, and 492 nm is measured by galvanostatic anodization for 3600 s at 0.3, 0.4, 0.6, 0.7, and 1 $mAcm^{-2}$, respectively. As the current density increases, the thickness of the barrier oxide layer increases, whereas that of the porous layer decreases. As indicated above, the greater thickness of the barrier oxide layer at a higher current density is attributed to higher forming voltage, which usually determines the thickness of the barrier oxide. The dissolution of the outmost surface consisting of a porous layer is prompted at a high current density, resulting in a decreased

Table 1. Summary of the thickness of porous, barrier, and total layers in terms of current density and anodizing time

Current density ($mAcm^{-2}$)	Time (sec)	Thickness (nm)		
		Barrier	Porous	Total
0.05	3600	-	89	89
0.1	3600	-	162	162
	7200	-	196	196
	10800	-	174	174
	14400	-	181	181
	18000	-	166	166
0.2	3600	-	316	316
	7200	-	460	460
0.3	3600	144	181	325
0.4	900	85	85	170
	1800	149	121	270
	2700	212	166	378
	3600	243	166	409
0.6	1600	205	143	348
	3600	296	151	447
0.7	1300	250	136	386
	3600	311	143	454
1	3600	386	106	492

thickness of the porous layer.

Conclusions

We demonstrated that galvanostatic anodization of niobium at less than 3 $mAcm^{-2}$ produces typical porous type oxide, whereas a duplex oxide film consisting of thick porous and barrier oxide layers is formed at a higher current density. The total thickness of the duplex film increases as the current density increases. It is due to an increase in thickness of the barrier oxide, which is solely determined by the maximum voltage reached during anodization. A sudden voltage drop is observed immediately after reaching the maximum voltage, which is attributed to a leakage of current flow due to the breakdown of oxide films. Since the high forming voltage caused by high current density leads to massive movement of ions in the oxide, the collapse of nanosized pores occurs, resulting in the formation of large holes.

The mechanism of duplex structures is attributed to the mixture electrolyte of H_3PO_4 and HF. The barrier oxide layer is formed by anodization of H_3PO_4, whereas porous oxide is formed in HF. Relatively high voltage is required to move heavy PO_4^{3-} ions, compared to F^- ions. F^- ions are a sole contributor in forming the porous oxide at a low current density, whereas not only F^- but also PO_4^{3-} ions can start to play an important role in the formation of porous and barrier oxide layers, respectively, at a high current density.

Acknowledgments. This research was financially supported by the Ministry of Knowledge Economy (MKE), Korea Institute for Advancement of Technology (KIAT) through the Inter-ER Cooperation Projects (0000577).

References

1. Castro, A.; Millán, P.; Pardo, L.; Jiménez, B. *J. Mater. Chem.* **1999**, *9*, 1313.
2. Aegerter, M. A. *Sol. Energ. Mat. Sol. C* **2001**, *68*, 401.
3. Sayama, K.; Sugihara, H.; Arakawa, H. *Chem. Mat.* **1998**, *10*, 3825.
4. Matsuno, H.; Yokoyama, A.; Watari, F.; Uo, M.; Kawasaki, T. *Biomaterials* **2001**, *22*, 1253.
5. Miyazaki, T.; Kim, H.; Kokubo, T.; Ohtsuki, C.; Nakamura, T. *J. Ceram. Soc. Jpn.* **2001**, *109*, 929.
6. Lee, C.; Kwon, D.; Yoo, J. E.; Lee, B. G.; Choi, J.; Chung, B. H. *Sensors* **2010**, *10*, 5160.
7. Tauseef Tanvir, M.; Aoki, Y.; Habazaki, H. *Thin Solid Films* **2009**, *517*, 6711.
8. Yoo, J. E.; Choi, J. *Electrochem. Commun.* **2011**, *13*, 298.
9. Kominami, H.; Oki, K.; Kohno, M.; Onoue, S.; Kera, Y.; Ohtani, B. *J. Mater. Chem.* **2001**, *11*, 604.
10. Torres, J. D.; Faria, E. A.; SouzaDe, J. R.; Prado, A. G. S. *J. Photochem. Photobiol. A* **2006**, *182*, 202.
11. Xie, Y.; Li, Z.; Xu, Z.; Zhang, H. *Electrochem. Commun.* **2011**, *13*, 788.
12. Choi, J.; Lim, J. H.; Lee, S. C.; Chang, J. H.; Kim, K. J.; Cho, M. A. *Electrochim. Acta* **2006**, *51*, 5502.
13. Robert, L. K. *Electrochem. Commun.* **2005**, *7*, 1190.
14. Lim, J. H.; Park, G.; Choi, J. *Curr. Appl. Phys.* **2012**, *12*, 155.
15. Nielsch, K.; Choi, J.; Schwirn, K.; Wehrspohn, R. B.; Gösele, U. *Nano Lett.* **2002**, *2*, X.
16. Patermarakis, G.; Papandreadis, N. *Electrochim. Acta* **1993**, *38*, 2351.
17. Shawaqfeh, A. T.; Baltus, R. E. *J. Electrochem. Soc.* **1998**, *145*, 2699.
18. Ono, S.; Saito, M.; Ishiguro, M.; Asoh, H. *J. Electrochem. Soc.* **2004**, *151*, B473.
19. Ono, S.; Saito, M.; Asoh, H. *Electrochim. Acta* **2005**, *51*, 827.
20. Montero-Moreno, J. M.; Sarret, M.; Müller, C. *Micropor. Mesopor. Mat.* **2010**, *136*, 68.
21. Patermarakis, G.; Moussoutzanis, K. *J. Electroanal. Chem.* **2011**, *659*, 176.
22. Xie, Y.; Li, Z.; Xu, H.; Xie, K.; Xu, Z.; Zhang, H. *Electrochem. Commun.* doi: 10.1016/j.elecom.2012.01.021.
23. Diggle, J. W.; Downie, T. C.; Coulding, C. W. *Chem. Rev.* **1969**, *69*, 365-405.